Projections for the length of tree-ring growing season on the Tibetan Plateau derived from CMIP5 model output

Abstract: Response of vegetation growing season to global warming during the 20th century has attracted much attention. How the growing season will change during the next century is the basic information for evaluating the consequences of global warming, especially on the Tibetan Plateau (TP) where the warming trend is much more significant than the global mean. In this study, a long-term (1960–2014) averaged mean length of tree-ring growing season (LOS) on the TP was derived from results of VS-Oscilloscope model. Bootstrap correlations reveal previous September to current September mean and minimum temperature all significantly ($p < 0.05$) and positively affect LOS during the period 1960–2014. Although March–May precipitation also significantly affect LOS, partial correlation further reveal that April–September minimum temperature is the strongest factor for LOS in the study region during the past 55 years. Based on this relationship, we predicted the variability of tree-ring growing season on the TP under three emission scenarios (Representative Concentration Pathways (RCP) 2.6, RCP 6.0 and RCP 8.5) from 17 earth system models participating in the Coupled Model Intercomparison Project Phase 5 (CMIP5). Results show a general increase of the length of tree-ring growing season over the 21st century under the selected three emission scenarios. By the middle of this century, LOS will extend by about three and four weeks under RCP 2.6 and RCP 6.0 scenarios, and by more than one month (~37 days) under RCP 8.5 scenario, relative to the baseline period 1960–2014. By around 2100, it will extend by ~17 days under RCP 2.6, ~50 days under RCP 6.0, and ~82 days under RCP 8.5. An averaged extension rate of 0.21 day/year, 0.36 day/year and 0.50 day/year is detected from 2015 to 2100 under the three scenarios from low to high, respectively. Definitely, such theoretical extension may be disturbed by other factors, such as nitrogen limitation, our results nevertheless provide the first scenario of the length of tree-ring growing season for the next almost one hundred years on the TP.

Key words: length of tree-ring growing season (LOS), temperature sensitivity, Representative Concentration Pathways (RCPs), CMIP5, Tibetan Plateau

1. Introduction

Response of vegetation growing season to global warming has attracted much attention during the past decades (Linderholm, 2006; Xia et al., 2015). A number of previous studies have reported extension of growing season for different regions

(Fernández-Long et al., 2013; Linderholm et al., 2008; Qian et al., 2010; Spinoni et al., 2015). For example, based on a datasets of 1263 phenological time series from 112 vegetation species in China (Ge et al., 2015), results demonstrated that 90.8% of the vegetation starting dates had advanced and 69.0% of the ending records had delayed trend from 1960 to 2011. On the Tibetan Plateau, satellite remote sensing data revealed widespread advance in the start of vegetation growing season during the 1980s and 1990s but substantial delay over 2000–2011 in the southwest region (Shen et al., 2015). Such phenological changes are likely to influence the distribution of plant species (Chuine, 2010), or may change carbon uptake and potentially mitigate climate change (Dragoni et al., 2011; Peñuelas et al., 2009).

Considering forests play a key role in the global carbon cycle and sequestration of carbon emissions derived from fossil fuels (Way and Oren, 2010), it's more ecological-related important to investigate forest growing season under current or future climate change scenario. As previous study indicated, a longer tree growing season may indicate more carbon available allocate to growth because respiration acclimated more strongly than photosynthesis (Way and Oren, 2010), increasing carbon assimilation but moderating carbon losses. However, on the other hand, a longer growing season may not directly accelerate tree stem radial growth (wood) but followed different developmental trajectories, such as, allocating more biomass to leaves or roots and growing taller for a given stem diameter. Therefore, considering the growth of tree organs does not solely depend on the fueling of carbon but, rather, is at least transitorily an active process modulated by seasonal variations in the ability of the organ to grow (Dietze et al., 2014; Fatichi et al., 2014), more individual detailed process of organ growth, such as, leaf and wood, is expected. Accordingly, a great progress of leaf phenology, either for the past six decades or for the future, has achieved over the past several years (Fu et al., 2015; Ge et al., 2014; Juknys et al., 2016; Piao et al., 2015). However, the growth process of wood (tree-ring) for a long-term period has received less attention (Delpierre et al., 2015), even though it likely influences the overall plant functioning and fitness.

Nevertheless, it's already well known that the response of wood/tree-ring growth to climate change and the shift in timing of different phenological phases is a result of the integrated impact of different factors, such as temperature, length of photoperiod, nutritive conditions, and precipitation (Chuine et al., 2010; Delpierre et al., 2015; Körner and Basler, 2010; Morin et al., 2010). Among these factors, temperature is expected to be a main driver for the phenology of xylogenesis (Moser et al., 2010; Prislan et al., 2013; Rossi et al., 2008), considering its direct influence on cell structure (Begum et al., 2012), and/or on the basic processes of modulate the division rate of cambium initials (Begum et al., 2013), and the regulation of gene expression related to active auxin transport (Schrader et al., 2003). Still, as it was emphasized by (Polgar and Primack, 2011), the dominant role of temperature in the development of plants makes them excellent indicators of global warming. Alternatively, other related studies (Jeong et al., 2011; Shen et al., 2014; Xia et al., 2015) also indicate that an appropriate combination of monthly temperatures may be used as a proxy of the vegetation growing season when phenological data are not available for the past or for

the future in different study regions.

With an average elevation of more than 4000 m a.s.l., the Tibetan Plateau (TP) is considered as the “Third Pole” of the earth (Yao et al., 2013). Its special geographic locations motivated a large member of studies focused in the region. However, most of them are assessing historical changes of vegetation growing season (Chen et al., 2015; Shen et al., 2015; Yi and Zhou, 2011; Yu et al., 2010; Zhang et al., 2013) either extracted from remote-sensing observations or from in-situ ground observations. Recently, with an innovative approach based on tree-ring data, a unique long-term record of vegetation phenological variability over the period 1960–2014 was available for the TP (Yang et al., 2017). However, there has been a shortage of studies predicting future changes for the region. According to the Fifth Assessment Report of the Intergovernmental Panel on Climate Change (IPCC AR5) (IPCC, 2013), increasing in the concentrations of anthropogenic atmospheric green-house gas is very likely result in the observed global warming since 1950, and which is almost certain to continue in the future. Hence, how the growing season will change during the next century is the basic information for evaluating the consequences of global warming.

Compared to the other climate models (Reichler and Kim, 2008), substantial improvements have been achieved to the state-of-the-art Coupled Model Intercomparison Project Phase 5 (CMIP5) simulations (Knutti and Sedláček, 2013). CMIP5 is based on the projected population growth, technological development, and societal responses in the future (Moss et al., 2010; van Vuuren et al., 2011). The advantages of the CMIP5 are: more complex models run at higher resolution; more complete representations of external forcings; more types of scenario and more diagnostics stored (Knutti and Sedláček, 2013). Additionally, the individual Representative Concentration Pathways (RCP) scenarios of the CMIP5 provide a rough estimate of the fixed radiative forcing (Taylor et al., 2012). For example, the radiative forcing in RCP 8.5 increases throughout the 21st century before reaching a level of about 8.5 W m^{-2} at the end of this century. In addition to this “high” scenario, there are two intermediate scenarios, RCP 4.5 and RCP 6.0, and a low scenario, RCP 2.6, in which radiative forcing reaches a maximum near the middle of the 21st century before decreasing to an eventual nominal level of 2.6 W m^{-2}. Accordingly, the outputs of CMIP5 climate models could provide a better way for studying possible changes of climate for the future.

To sum up, in this study, we intend to use the outputs of CMIP5 to predict length of tree-ring growing season on the Tibetan Plateau. To the best of our knowledge, our study is among the first to conduct the assessment of future growing season based on CMIP5 outputs for the next almost one hundred years. The aim of this study is to: (1) quantify the relationship between length of tree-ring growing season and temperature variability based on observational data during 1960–2014; (2) evaluate the performance of CMIP5 coupled models by comparing the observed changes and the simulated results for the historical period 1960–2005; (3) reveal the possible changes in the growing season for 2015–2100 under three RCP scenarios (RCP 2.6, RCP 6.0 and RCP 8.5) in the study region.

2 Materials and methods

2.1 Study region and tree-ring phenological data

Our sampling sites are located on the Tibetan Plateau (Fig.1). Averaged from 20 meteorological stations data during the period 1960–2014 (Fig.S1), the mean annual temperatures is 4.3ºC and mean annual precipitation is 518.7mm. July is the hottest month (14.2ºC) and January is the coldest one (–7.3ºC). April–September precipitation accounts for 88.2% of the annual precipitation. During the past six decades, significant ($p < 0.01$) warming trends have been observed over the study region (Table S1 and Fig.S2). The linear trends of the mean annual and growing season (April–September) minimum temperatures are 0.36 day/decade and 0.28 day/decade, respectively. The non-growing season (previous October to current March) temperature and precipitation also significantly increased during the past 55 years. However, the April–September precipitation shows insignificant ($p = 0.23$) variability from 1960 to 2014.

Tree-ring phenological data was derived from results of process-based Vaganov-Shashkin (VS) model (Shashkin and Vaganov, 1993; Vaganov, 1996a). VS model was developed to quantify tree-ring formation as a function of climate and environmental variables, by using a limited number of equations relating daily temperature, precipitation, and sunlight to the kinetics of secondary xylem development (Vaganov, 1996b; Vaganov et al., 2011). In this study, we used the recently updated version of the VS model: VS-Oscilloscope (Shishov et al., 2016), which allows the simulation of tree-ring growth more physiological-meaning and can be easily used by researchers because of its visual approach (http://vs-genn.ru/downloads/). Start of tree-ring growing season (SOS) is defined as the time of first xylem cell differentiation and end of growth (EOS) as the time of last xylem cell differentiation. Length of tree-ring growing season (LOS) is calculated as the difference of EOS and SOS for each year. Based on the successful simulation of tree-ring width series across the study region (more detailed information can be referred to (Yang et al., 2017)), we averaged all the derived LOS series to represent phenological variability of tree-ring formation for the entire plateau region.

2.2 Relationships between tree-ring phenology and climate

Bootstrap correlation between tree-ring phenological series and monthly temperature (including mean, minimum and maximum temperature) and precipitation data was calculated with the program DENDROCLIM2002 (Biondi and Waikul, 2004). This analysis was conducted from previous September to current September during the period 1960–2014. Relationships between seasonal or annual assembled climate data and LOS were calculated to extract the most significant factor. Furthermore, we performed partial correlation to eliminate the possible linear relationships among the climate data. The extracted strongest climate factor was used to predict the variability of LOS for the future.

2.3 CMIP5 models

We used the CMIP5 full set general circulation models, which includes multiple realizations of each model. Selecting this option gives slightly smoother probability density functions at the expense of much more computer time (van Oldenborgh et al., 2013). Monthly outputs of the CMIP5 models were downloaded from the Program for Climate Model Diagnosis and Intercomparison (PCMDI) server: Earth System Grid Federation (http://cmip-pcmdi.llnl.gov/cmip5). The selected coordinates represent our study region are 27 ºN–40 ºN, 85–105ºE.

Considering most of the instrumental records on the TP started after the year 1960, we compared the variance of climate between model outputs and observed one during the "historical" period 1960–2005, to test the representation of models in the study region. According to that, 17 CMIP5 models were selected in this study (Table 1). The other models failed to reproduce the current April–September minimum temperature in the study region, gave severely biased simulated temperature trends during the historical period. For each model, we use the individual result from all the available realizations instead of the ensemble mean over the realizations. This is considered because each ensemble member has its own internal variability and the inter-annual variation of the ensemble mean would be reduced compared to one individual simulation (Anav et al., 2013).

We selected three RCP scenarios: RCP 2.6, RCP 6.0 and RCP 8.5, to represent different future CO_2 and radiative forcing scenarios from low to high, respectively (Jones et al., 2013; Taylor et al., 2012). Not every model ran all RCP scenarios (Table 1). Accordingly, 15 models were used for RCP 2.6, 13 models for RCP 6.0 and 16 models for RCP 8.5 scenarios. Model runs were analyzed to the year 2100. The average of multiple models performs better than any single model when compared with observations (Gleckler et al., 2008; Reichler and Kim, 2008), so we averaged all the related models to represent "historical" and "prediction" climate under the three scenarios of RCP 2.6, RCP 6.0 and RCP 8.5.

3. Results

3.1 Relationships between tree-ring phenology and climate

The averaged mean length of tree-ring growing season (LOS) is 103 days during the period 1960–2014, with a standard deviation of 20 days in the study region (Fig.2a). A significant ($p < 0.01$) extension of LOS was detected, with a linear trend of 0.46 day/year during the past 55 years. Bootstrap correlation (Fig.3) show significant ($p < 0.05$) relationships between LOS and mean, maximum as well as minimum temperature from previous September to current September (except in current May with maximum temperature) during the past 55 years. Such consistent positive relationships indicate the strong influence of temperature on LOS: a warmer temperature probably results in a longer growing season in the study region.

Additionally, we detected prominent ($p < 0.05$) correlations between LOS and current March to May precipitation. However, partial correlations further reveal that April–September minimum temperature is the strongest factor for LOS during the past 55 years (r = 0.80, $p < 0.01$, 1960–2014) (Fig.2b). Accordingly, we established a linear regression function

$$LOS = 13.23 \times Tmin_{\text{April–September}} + 36.44$$

to predict length of tree-ring growing season in the future.

3.2 Projected changes in climate

The 17 multi-model ensemble means shows the averaged April–September minimum temperature is 9.54°C while the observed one is 4.85°C during the "historical period" 1960–2005. Apart from this absolute difference, we found the ensemble model means reveal similar year-by-year variance to the observed one (Fig.4), with a significant ($p < 0.01$) correlation of 0.81 during the common period 1960–2005. Their first-order differenced series (r = 0.50) also reach the significance level of $p < 0.01$. Additionally, almost the same linear trends were detected between the observations and the simulations during this "historical period". The linear increasing trend for the observations is 0.225°C/10year, while the trend is 0.229°C/10year for the 17 ensemble model output (with 5%–95% uncertainty intervals of 0.247°C to 0.211°C/10 year) over the common 46 years. Hence, we are confident that all the available models have the ability to predict April–September minimum temperature changes on the plateau for the 21st century. Anyway, considering the absolute difference between the predictions and observations during the "historical period", we subtracted the value of 4.69°C from the model outputs for the prediction.

The projection of climatic parameters for TP on the basis of 17 global circulation models (Fig.S3 and Table S2) show rising near surface temperature in April–September compared to the historical baseline period (1960–2005). The ensembles mean changes under the optimistic climate change scenario RCP 2.6 tends to increase by ~1.50°C during middle of the 21st century. Thereafter, temperature fluctuates at around this level until the end of this century. In total, the increased temperature is less than 2.0°C under this scenario for the 21st century. Under the intermedium scenario RCP 6.0, April–September minimum temperature tends to increase by 2.0°C at around 2040, and then, it keeps almost stable for a continuous 20 years. From 2060 onwards, temperature continued to increase and exceed a level of 4.0°C than the historical period at the end of this century. Under the pessimistic scenario RCP 8.5, temperature raises by ~2.0°C at the year 2035. A continuous increasing trend is detected thereafter, and which result in a mean temperature higher ~6.0°C than 1960–2005 at the end of the 21st century.

3.3 Projected changes of tree-ring growing season

According to the different climate change scenarios and global circulation models for the future, the extension in the projected length of tree-ring growing season in relation

to that for the period 1960–2014 is presented in Fig.5. The predicted LOS shows sustained extension trends with the rate of 0.45 day/year during the period 2015–2050 under the RCP 2.6 scenario, resulting in the corresponding extension of about 16.4 days. After the middle of the 21st century, the extended rate (0.37 day/year) is reduced and almost keeps stable from 2060 to 2100. Over the full predicted period 2015–2100, the extension is about half a month with the mean averaged rate of 0.21 day/year under this optimistic scenario. More detailed anticipated days of the LOS during the 21st century are listed in Table 3. Under the RCP 6.0 scenario, LOS sustains an extension rate of 0.36 day/year from 2015 to 2100. On average, about one and half months will be extended at the end of this century. Compared to the observation period 1960–2014, length of tree-ring growing season will be extended about 82 days under RCP 8.5 scenario at the end of this predicted century. The mean averaged extend rate is 0.50 day/year under this pessimistic scenario. In Fig.5, we also present the corresponding 5%–95% uncertainty intervals calculated from the multiple models, which shows large uncertainties among the different models under the three scenarios. Nevertheless, our results provide valuable information about general trends on ongoing and projected climate-related changes in the length of tree-ring growing season on the Tibetan Plateau.

4. Discussion

4.1 Relationships between tree-ring phenology and climate

Although meteorological stations are normally locate at the valley region while tree-ring sampling sites are generally concentrated in the mountains on the Tibetan Plateau, available results confirmed the reliability of utilizing climatic records from valley bottoms to calibrate tree-ring records in mountainous region (Zeng and Yang, 2016). During the period 1960–2014, we observed significantly ($p < 0.01$) increased temperature but insignificant ($p = 0.23$) variability of precipitation in the growing season of April–September (Fig.S2 and Table S1). This may indicate likely intensified drought stress during the growing season in the study region. However, significant extension of the length of tree-ring growing season was detected from 1960 to 2014. Definitely, the strongest factor for the LOS is April–September minimum temperature while the influence of precipitation is week, warming temperature therefore result in extension of LOS in the study region is rational. Consistently, some studies also indicated that the lengthened growing season of different tree species was probably driven by the warming temperature (Lange et al., 2016; Moser et al., 2010; Peñuelas et al., 2009). Firstly, we speculate that such probably intensified drought stress does not reach the threshold to negatively affect tree-ring phenology variability during the past 55 years. Secondly, we hypothesize that previous winter season and/or pre-growing season precipitation may supply the available soil moisture for tree-ring formation in the study region, because we also detected significantly ($p < 0.01$) increased precipitation during October–March. Thirdly, the seasonal amount of precipitation is not equal to soil moisture that tree-ring growth directly needed. As

evidenced by the VS-oscilloscope, significantly ($p < 0.10$) increased soil moisture content but insignificant trend of precipitation was found during April–July for the period 1960–2008 in the study region (He et al., 2017). Moreover, previous results showed strong and positive correlations between large-scale TP surface temperature anomaly in prior winter (October–February) and current April–June moisture availability on the southeaster TP (Li et al., 2016). Accordingly, the co-variability of warming and wetting trend, to some extent, may occur in the study region. Hence, length of tree-ring growing season may benefit from the predicted warming trend of future climate change scenario on the TP, although the complicated interactions between chilling, temperatures and photoperiod were still not completely resolved (Chuine et al., 2010; Hanninen and Tanino, 2011; Körner and Basler, 2010).

4.2 Predicted length of tree-ring growing season

As far as we know, it's the first study to predict length of tree-ring growing season based on a long-term baseline period 1960–2014 on the Tibetan Plateau. We thus provide valuable information of vegetation growing season for the future in the study region, where it is considered both sensitive (Yao et al., 2013) and vulnerable (Xu et al., 2009) to climate change. As shown in Fig.5, LOS is predicted to extend by about 21, 27 and 37 days in the middle of the 21st century under RCP 2.6, RCP 6.0 and RCP 8.5 scenarios, respectively. In the Czech Republic and Austria, thermal growing season was anticipated to lengthen by 8–30 days based on three climate models of HadCM, ECHAM, and NCAR-PCM by 2050 (Trnka et al., 2011). Projections up to 2050 indicate that the growing season may increase by 3 to 4 weeks at most of the stations based on the ECHAM4/OPYC3 AOGCM model in Nordic Arctic (Førland et al., 2004). The two studies are therefore in general consistent with our predicted results although based on different models and in various study regions. However, contrary to our extended days of 21–60 by the 2080s, projections of two reginal climate models (PRECIS and RegCM3) under A1B emission scenario for China revealed a prolongation of thermal growing season (above 10 ºC) by up to more than 100 days by that time period (Tian et al., 2014). Definitely, the different predicted regions as well as the different definitions for the thermal growing season and our tree-ring phenology variability probably result in the inconsistent results. Secondly, the discrepancy is partly due to the differences of temperature changes between the RCP scenarios and the previous versions of the scenarios. Thirdly, the limited number of models used by this study (Tian et al., 2014) may also result in some bias. Because we found in general consistent results either according to 23 multi-model mean of simulations for the majority of Europe (Ruosteenoja et al., 2016), or based on 19 CMIP phase 3 global climate models in Finland (Ruosteenoja et al., 2011). By the end of this century, about 1.5 to 2 months prolongation of thermal growing season was predicted by the two studies. Consequently, we recommend that multiple models ensemble means are more precisely for the projection of length of growing season under the changing climate for different study regions.

In contrary to the overall extension of vegetation growing season on the Northern

Hemisphere as discussed above, a shorter growing season in the future under RCP 8.5 scenario based on regional climate model projections at 30-km resolution over Malawi south of 13.5°S was predicted (Vizy et al., 2015). As indicated by their results, the growing season length was spatially predicted to be 5–55 days shorter by the middle of 21st century. By the end of this century, the length was anticipated to be 20–70 days shorter with significant differences extending into northern Malawi. However, no related study is available to compare with their results at present. Consequently, compared to the general extension of the vegetation growing season during the 21st century in the Northern Hemisphere, whether the predicted shortened growing season is a result of the different methods used, or is a result from the characteristics of local climate condition in the Southern Hemisphere of Malawi, is still inconclusive and expects more related researches in the future.

5. Conclusion

This study investigated the possible changes in the length of tree-ring growing season on the Tibetan Plateau during the 21st century, based on the sensitivity of LOS and April–September minimum temperature projections under three RCP scenarios from the latest state-of-the-art CMIP5. Compared to the baseline period 1960–2014, a general extension of LOS is predicted under RCP 2.6, RCP 6.0 and RCP 8.5 scenarios over the period 2015–2100. The optimistic scenario RCP 2.6 shows two to three weeks extension of the growing season during the 21st century. The intermediate and pessimistic scenarios of RCP 6.0 and RCP 8.5 indicate a constant extended rate and which result in the prolongations of ~50 and ~82 days at the end of the 21st century.

Definitely, such theoretically extension of length of tree-ring growing season may be interrupted by other environmental factors, such as, increased demand for soil resources because of a longer photosynthetically active period in conjunction with other global change factors might exacerbate resource limitation (Elmore et al., 2016). A longer growing season may also result in the introduction of other new plants or new insects. Problems may therefore occur, such as damage caused by increased numbers of insects as well as a higher risk of plant disease (Engen-Skaugen and Tveito, 2004). More complicatedly, some studies (Lange et al., 2016; Morin et al., 2010) even revealed the nonlinear relationships between phenological variability of trees and climate data and therefore suggested that predictions of phenological changes in the future should not be built on extrapolations of current observed trends, although the relationship between temperature and most phenological phases of xylogenesis was clearly linear as reported by (Rossi et al., 2014). Nevertheless, we expect more complicated tree-physiological and climate models to deeply investigate it in the next step.

Acknowledgements

This study was jointly funded by the National Natural Science Foundation of China

(Grant No. 41520104005, 41325008). Minhui He appreciates the support by the Alexander von Humboldt Foundation.

References:

Anav A, Friedlingstein P, Kidston M, Bopp L, Ciais P, Cox P, Jones C, Jung M, Myneni R, Zhu Z (2013) Evaluating the Land and Ocean Components of the Global Carbon Cycle in the CMIP5 Earth System Models. Journal of Climate 26:6801-6843.

Begum S, Nakaba S, Yamagishi Y, Oribe Y, Funada R (2013) Regulation of cambial activity in relation to environmental conditions: understanding the role of temperature in wood formation of trees. Physiologia plantarum 147:46-54.

Begum S, Shibagaki M, Furusawa O, Nakaba S, Yamagishi Y, Yoshimoto J, Jin HO, Sano Y, Funada R (2012) Cold stability of microtubules in wood-forming tissues of conifers during seasons of active and dormant cambium. Planta 235:165-179.

Biondi F, Waikul K (2004) DENDROCLIM2002: A C++ program for statistical calibration of climate signals in tree-ring chronologies. Computers & Geosciences 30:303-311.

Chen X, An S, Inouye DW, Schwartz MD (2015) Temperature and snowfall trigger alpine vegetation green-up on the world's roof. Global change biology 21:3635-3646.

Chuine I (2010) Why does phenology drive species distribution? Philos Trans R Soc Lond B Biol Sci 365:3149-3160.

Chuine I, Morin X, Bugmann H (2010) Warming, photoperiods, and tree phenology. Science 329:277-278.

Delpierre N, Vitasse Y, Chuine I, Guillemot J, Bazot S, Rutishauser T, Rathgeber CBK (2015) Temperate and boreal forest tree phenology: from organ-scale processes to terrestrial ecosystem models. Annals of Forest Science.

Dietze MC, Sala A, Carbone MS, Czimczik CI, Mantooth JA, Richardson AD, Vargas R (2014) Nonstructural carbon in woody plants. Annual review of plant biology 65:667-687.

Dragoni D, Schmid HP, Wayson CA, Potter H, Grimmond CSB, Randolph JC (2011) Evidence of increased net ecosystem productivity associated with a longer vegetated season in a deciduous forest in south-central Indiana, USA. Global change biology 17:886-897.

Elmore AJ, Nelson DM, Craine JM (2016) Earlier springs are causing reduced nitrogen availability in North American eastern deciduous forests. Nature plants 2:16133.

Engen-Skaugen T, Tveito OE (2004) Growing-season and degree-day scenario in Norway for 2021–2050. Clim. Res. 26:221-232.

Førland EJ, Skaugen TE, Benestad RE, Hanssen-Bauer I, Tveito OE (2004) Variations in thermal growing, heating, and freezing indices in the Nordic Arctic, 1900–2050. Arctic, Antarctic, and Alpine Research 36:347-356.

Fatichi S, Leuzinger S, Körner C (2014) Moving beyond photosynthesis: fromcarbon source to sink-driven vegetation modeling. New Phytologist 201:1086-1095.

Fernández-Long ME, Müller GV, Beltrán-Przekurat A, Scarpati OE (2013) Long-term and recent changes in temperature-based agroclimatic indices in Argentina. International Journal of

Climatology 33:1673-1686.
Fu YH, Zhao H, Piao S, Peaucelle M, Peng S, Zhou G, Ciais P, Huang M, Menzel A, Penuelas J, Song Y, Vitasse Y, Zeng Z, Janssens IA (2015) Declining global warming effects on the phenology of spring leaf unfolding. Nature 526:104-107.
Ge Q, Wang H, Dai J (2014) Simulating changes in the leaf unfolding time of 20 plant species in China over the twenty-first century. International journal of biometeorology 58:473-484.
Ge Q, Wang H, Rutishauser T, Dai J (2015) Phenological response to climate change in China: a meta-analysis. Global change biology 21:265-274.
Gleckler PJ, Taylor KE, Doutriaux C (2008) Performance metrics for climate models. Journal of Geophysical Research 113: D06104.
Hanninen H, Tanino K (2011) Tree seasonality in a warming climate. Trends in plant science 16:412-416.
He M, Shishov V, Kaparova N, Yang B, Bräuning A, Grießinger J (2017) Process-based modeling of tree-ring formation and its relationships with climate on the Tibetan Plateau. Dendrochronologia 42:31-41.
IPCC (2013) Climate change 2013: the physical science basis. Contribution of working group I to the fifth assessment report of the intergovernmental panel on climate change. T. F. Stocker et al., Eds., Cambridge University Press, Cambridge, United Kingdom and New York, NY, USA, 1535 pp.
Jeong S-J, Ho C-H, Gim H-J, Brown ME (2011) Phenology shifts at start vs. end of growing season in temperate vegetation over the Northern Hemisphere for the period 1982-2008. Global change biology 17:2385-2399.
Jones C, Robertson E, Arora V, Friedlingstein P, Shevliakova E, Bopp L, Brovkin V, Hajima T, Kato E, Kawamiya M, Liddicoat S, Lindsay K, Reick CH, Roelandt C, Segschneider J, Tjiputra J (2013) Twenty-First-Century Compatible CO2Emissions and Airborne Fraction Simulated by CMIP5 Earth System Models under Four Representative Concentration Pathways. Journal of Climate 26:4398-4413.
Juknys R, Kanapickas A, Sveikauskaite I, Sujetoviene G (2016) Response of deciduous trees spring phenology to recent and projected climate change in Central Lithuania. International journal of biometeorology 60:1589-1602.
Körner C, Basler D (2010) Phenology under global warming. Science 327:1461-1462.
Knutti R, Sedláček J (2013) Robustness and uncertainties in the new CMIP5 climate model projections. Nature Climate Change 3:369-373.
Lange M, Schaber J, Marx A, Jackel G, Badeck FW, Seppelt R, Doktor D (2016) Simulation of forest tree species' bud burst dates for different climate scenarios: chilling requirements and photo-period may limit bud burst advancement. International journal of biometeorology 60:1711-1726.
Li J, Shi J, Zhang DD, Yang B, Fang K, Yue PH (2016) Moisture increase in response to high-altitude warming evidenced by tree-rings on the southeastern Tibetan Plateau. Climate Dynamics.
Linderholm HW (2006) Growing season changes in the last century. Agricultural and Forest Meteorology 137:1-14.
Linderholm HW, Walther A, Chen D (2008) Twentieth-century trends in the thermal growing season in the Greater Baltic Area. Climatic Change 87:405-419.
Morin X, Roy J, Sonie L, Chuine I (2010) Changes in leaf phenology of three European oak species in response to experimental climate change. The New phytologist 186:900-910.

Moser L, Fonti P, Buntgen U, Esper J, Luterbacher J, Franzen J, Frank D (2010) Timing and duration of European larch growing season along altitudinal gradients in the Swiss Alps. Tree Physiol 30:225-233.

Moss RH, Edmonds JA, Hibbard KA, Manning MR, Rose SK, van Vuuren DP, Carter TR, Emori S, Kainuma M, Kram T, Meehl GA, Mitchell JF, Nakicenovic N, Riahi K, Smith SJ, Stouffer RJ, Thomson AM, Weyant JP, Wilbanks TJ (2010) The next generation of scenarios for climate change research and assessment. Nature 463:747-756.

Peñuelas J, Rutishauser T, Filella I (2009) Phenology feedbacks on climate change. Science 324:887–888.

Piao S, Tan J, Chen A, Fu YH, Ciais P, Liu Q, Janssens IA, Vicca S, Zeng Z, Jeong SJ, Li Y, Myneni RB, Peng S, Shen M, Penuelas J (2015) Leaf onset in the northern hemisphere triggered by daytime temperature. Nat Commun 6:6911.

Polgar CA, Primack RB (2011) Leaf-out phenology of temperate woody plants: from trees to ecosystems. The New phytologist 191:926-941.

Prislan P, Gričar J, de Luis M, Smith KT, Čufar K (2013) Phenological variation in xylem and phloem formation in Fagus sylvatica from two contrasting sites. Agricultural and Forest Meteorology 180:142-151.

Qian B, Zhang X, Chen K, Feng Y, O'Brien T (2010) Observed Long-Term Trends for Agroclimatic Conditions in Canada. Journal of Applied Meteorology and Climatology 49:604-618.

Reichler T, Kim J (2008) How well do coupled models simulate today's climate? Bulletin of the American Meteorological Society 89:303-311.

Rossi S, Deslauriers A, Griçar J, Seo J-W, Rathgeber CBK, Anfodillo T, Morin H, Levanic T, Oven P, Jalkanen R (2008) Critical temperatures for xylogenesis in conifers of cold climates. Global Ecology and Biogeography 17:696-707.

Rossi S, Girard MJ, Morin H (2014) Lengthening of the duration of xylogenesis engenders disproportionate increases in xylem production. Global change biology 20:2261-2271.

Ruosteenoja K, Räisänen J, Pirinen P (2011) Projected changes in thermal seasons and the growing season in Finland. International Journal of Climatology 31:1473-1487.

Ruosteenoja K, Räisänen J, Venäläinen A, Kämäräinen M (2016) Projections for the duration and degree days of the thermal growing season in Europe derived from CMIP5 model output. International Journal of Climatology 36:3039-3055.

Schrader J, Baba K, May ST, Palme K, Bennett M, Bhalerao RP, Sandberg G (2003) Polar auxin transport in the wood-forming tissues of hybrid aspen is under simultaneous control of developmental and environmental signals. Proceedings of the National Academy of Sciences of the United States of America 100:10096-10101.

Shashkin AV, Vaganov EA (1993) Simulation model of climatically determined variability of conifers' annual increment (on the example of Scots pine in the steppe zone). Russ J Eco 24:275-280.

Shen M, Piao S, Dorji T, Liu Q, Cong N, Chen X, An S, Wang S, Wang T, Zhang G (2015) Plant phenological responses to climate change on the Tibetan Plateau: research status and challenges. National Science Review 2:1-14.

Shen M, Tang Y, Chen J, Yang X, Wang C, Cui X, Yang Y, Han L, Li L, Du J, Zhang G, Cong N (2014) Earlier-season vegetation has greater temperature sensitivity of spring phenology in northern hemisphere. PloS one 9:e88178.

Shishov VV, Tychkov II, Popkova MI, Ilyin VA, Bryukhanova MV, Kirdyanov AV (2016)

527 VS-oscilloscope: a new tool to parameterize tree radial growth based on climate conditions.
528 Dendrochronologia 39:42-50.
529 Spinoni J, Vogt J, Barbosa P (2015) European degree-day climatologies and trends for the period
530 1951-2011. International Journal of Climatology 35:25-36.
531 Taylor KE, Stouffer RJ, Meehl GA (2012) An Overview of CMIP5 and the Experiment Design.
532 Bulletin of the American Meteorological Society 93:485-498.
533 Tian Z, Yang X, Sun L, Fischer G, Liang Z, Pan J (2014) Agroclimatic conditions in China under
534 climate change scenarios projected from regional climate models. International Journal of
535 Climatology 34:2988-3000.
536 Trnka M, Eitzinger J, Semerádová D, Hlavinka P, Balek J, Dubrovský M, Kubu G, Štěpánek P, Thaler S,
537 Možný M, Žalud Z (2011) Expected changes in agroclimatic conditions in Central Europe.
538 Climatic Change 108:261-289.
539 Vaganov E (1996a) Analysis of a seasonal growth patterns of trees and modelling in dendrochronology.
540 Tree-Rings, Climate and Humanity (J. Dean, T. Swetnam, D. Meko, eds.), Radiocarbon:73-87.
541 Vaganov EA (1996b) Mechanisms and simulation modeling of tree-ring formation for conifers.
542 Lesovedenie 1:3-17.
543 Vaganov EA, Anchukaitis KJ, Evans MN (2011) How well understood are the processes that create
544 dendroclimatic records? A mechanistic model of the climatic control on conifer tree-ring growth
545 dynamics. In: Hughes, M.K. et al. (ed): Dendroclimatology, developments in paleoenvironmental
546 research Springer:37-75.
547 van Oldenborgh GJ, Doblas Reyes FJ, Drijfhout SS, Hawkins E (2013) Reliability of regional climate
548 model trends. Environmental Research Letters 8:014055.
549 van Vuuren DP, Edmonds J, Kainuma M, Riahi K, Thomson A, Hibbard K, Hurtt GC, Kram T, Krey V,
550 Lamarque J-F, Masui T, Meinshausen M, Nakicenovic N, Smith SJ, Rose SK (2011) The
551 representative concentration pathways: an overview. Climatic Change 109:5-31.
552 Vizy EK, Cook KH, Chimphamba J, McCusker B (2015) Projected changes in Malawi's growing
553 season. Climate Dynamics 45:1673-1698.
554 Way DA, Oren R (2010) Differential responses to changes in growth temperature between trees from
555 different functional groups and biomes: a review and synthesis of data. Tree Physiol 30:669-688.
556 Xia J, Yan Z, Jia G, Zeng H, Jones PD, Zhou W, Zhang A (2015) Projections of the advance in the start
557 of the growing season during the 21st century based on CMIP5 simulations. Advances in
558 Atmospheric Sciences 32:831-838.
559 Xu B, Cao J, Hansen J, Yao T, Joswia DR, Wang N, Wu G, Wang M, Zhao H, Yang W, Liu X, He J
560 (2009) Black soot and the survival of Tibetan glaciers. Proceedings of the National Academy of
561 Sciences of the United States of America 106:22114-22118.
562 Yang B, He M, Shishov V, Tychkov I, Vaganove E, Rossi S, Ljungqvist FC, Bräuning A, Grießinger J
563 (2017) New perspective on spring vegetation phenology and global climate change based on
564 Tibetan Plateau tree-ring data. PNAS.
565 Yao T, Masson-Delmotte V, Gao J, Yu W, Yang X, Risi C, Sturm C, Werner M, Zhao H, He Y, Ren W,
566 Tian L, Shi C, Hou S (2013) A review of climatic controls on δ18O in precipitation over the
567 Tibetan Plateau: Observations and simulations. Reviews of Geophysics 51:525-548.
568 Yi S, Zhou Z (2011) Increasing contamination might have delayed spring phenology on the Tibetan
569 Plateau. Proceedings of the National Academy of Sciences of the United States of America
570 108:E94; author reply E95.

Yu H, Luedeling E, Xu J (2010) Winter and spring warming result in delayed spring phenology on the Tibetan Plateau. Proceedings of the National Academy of Sciences of the United States of America 107:22151-22156.

Zeng Q, Yang B (2016) Comparing meteorological records between mountainous and valley bottom sites in the upper reaches of the Heihe River, northwestern China: implications for dendroclimatology. Theoretical and Applied Climatology.

Zhang G, Zhang Y, Dong J, Xiao X (2013) Green-up dates in the Tibetan Plateau have continuously advanced from 1982 to 2011. Proceedings of the National Academy of Sciences of the United States of America 110:4309-4314.

Figure and Table captions:

Fig.1 Study region, tree-ring sampling site and meteorological stations used in this study.

Fig.2 Mean length of tree-ring growing season (LOS) and their relationships with April–September minimum temperature during the period 1960–2014. The green bars are standard deviations derived from the different sampling sites. The red dash-dotted line is the linear trend of LOS for the past 55 years. The black dash-dotted line is the linear fitting trend between LOS and April–September minimum temperature.

Fig.3 Bootstrap correlations between LOS and climate factors from previous September to current September over the period 1960–2014. (a) correlations with mean temperature (Tmean); (b) correlations with maximum temperature (Tmax); (c) correlations with minimum temperature (Tmin); (d) correlations with precipitation (Pre). The insignificant ($p > 0.05$) correlations are marked with hollow histogram, while the significant ($p < 0.05$) correlations are demonstrated with filled color bars.

Fig.4 Comparison of the observed (black line) April–September minimum temperatures with results simulated (red line) by climate models under the historical period 1960–2005. Pink shaded bands show the 5% to 95% uncertainty range for these simulations from the 17 climate models.

Fig.5 LOS time series averaged over the Tibetan Plateau during 2015–2100 with respect to 1960–2014, projected by the CMIP5 models under the RCP 2.6, RCP 6.0, and RCP 8.5 scenarios. Negative (positive) values indicate the reduction (extension) in the number of days with respect to 1960–2014. The different colored shaded bands show the 5% to 95% uncertainty range for these simulations under the three RCP scenarios.

Table 1 Details of the CMIP5 models used in this study.

Table 2 Predicted LOS time series averaged (± standard deviation) over the Tibetan Plateau during 2015–2100 with respect to 1960–2014, projected by the CMIP5 models under the RCP 2.6, RCP 6.0 and RCP 8.5 scenarios.

Table 3 Predicted vegetation growing season by other studies.

Fig.S1 Monthly mean averaged climate conditions for the study region during the period 1960–2014. Tmean, Tmax, and Tmin indicate mean temperature, mean maximum temperature and mean minimum temperature, respectively. Pre means precipitation.

Fig. S2 Characteristics of mean temperature (Tmean), mean maximum temperature (Tmax), mean minimum temperature (Tmin) and precipitation during the past 55 years. The linear fitted series are also presented for the different climate factors during 1960–2014. Information for the detailed trends is listed in Table S1.

Fig.S3 Predicted April–September minimum temperature series under the three scenarios of RCP 2.6, RCP 6.0 and RCP 8.5 for 2006–2100. Temperature anomaly is calculated with respect to the "historical period" 1960–2005. The shaded bands show the 5% to 95% uncertainty range for these simulations under the three RCP scenarios.

Table S1 Linear trends of temperature and precipitation averaged from 20 meteorological stations data during the past 55 years (1960–2014) on the Tibetan Plateau (TP).

Table S2 Predicted April–September minimum temperature over the TP for the period 2006–2100 with respect to 1960–2005 (historical scenario), projected by the CMIP5 models under the RCP 2.6, RCP 6.0 and RCP 8.5 scenarios.

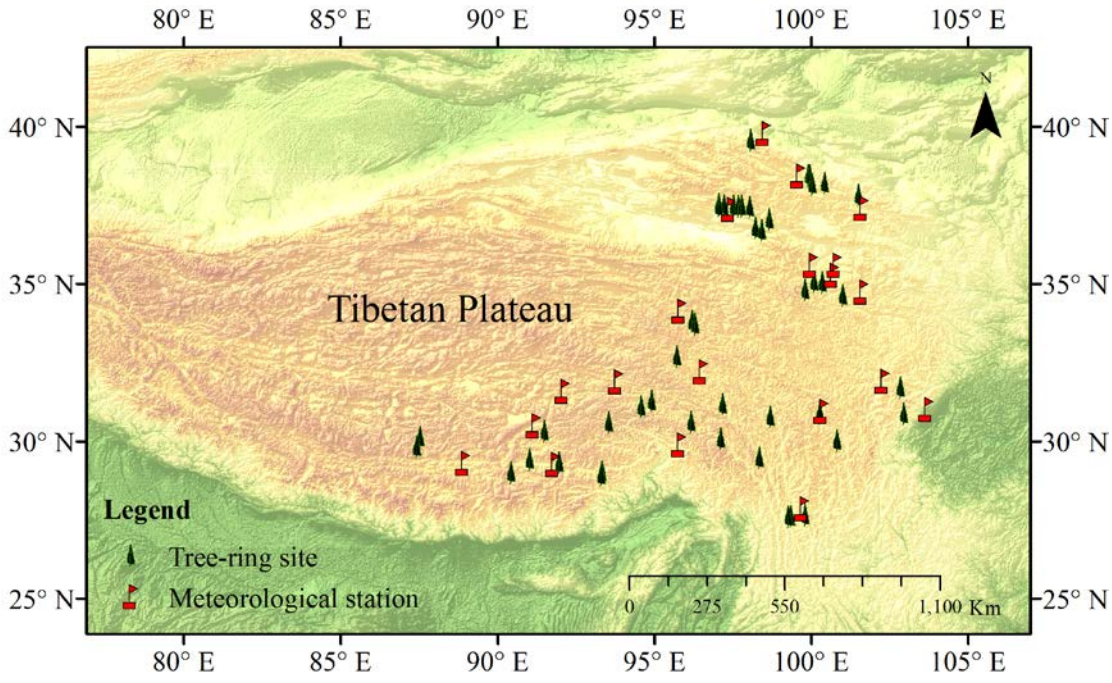

Fig.1 Study region, tree-ring sampling site and meteorological stations used in this study.

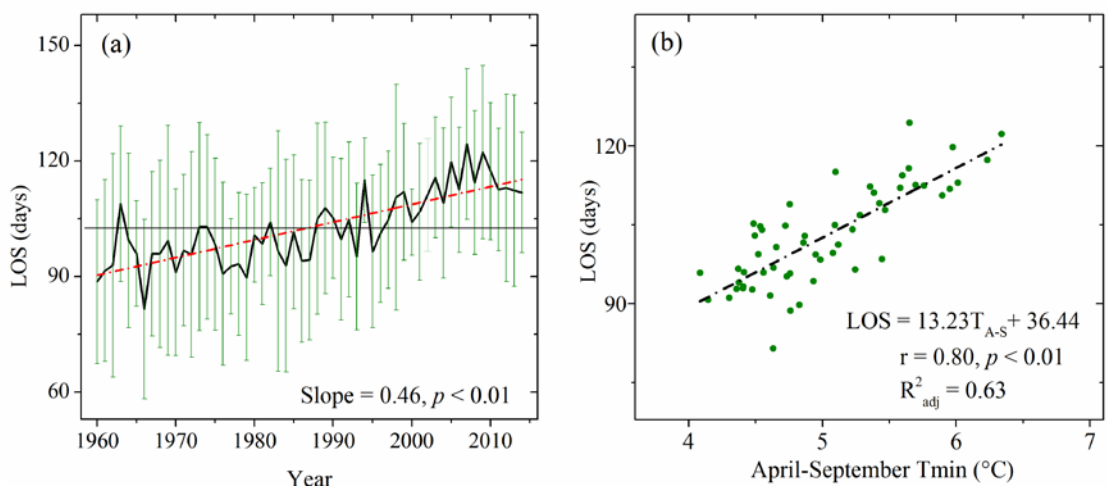

Fig.2 Mean length of tree-ring growing season (LOS) and their relationships with April–September minimum temperature during the period 1960–2014. The green bars are standard deviations derived from the different sampling sites. The red dash-dotted line is the linear trend of LOS for the past 55 years. The black dash-dotted line is the linear fitting trend between LOS and April–September minimum temperature.

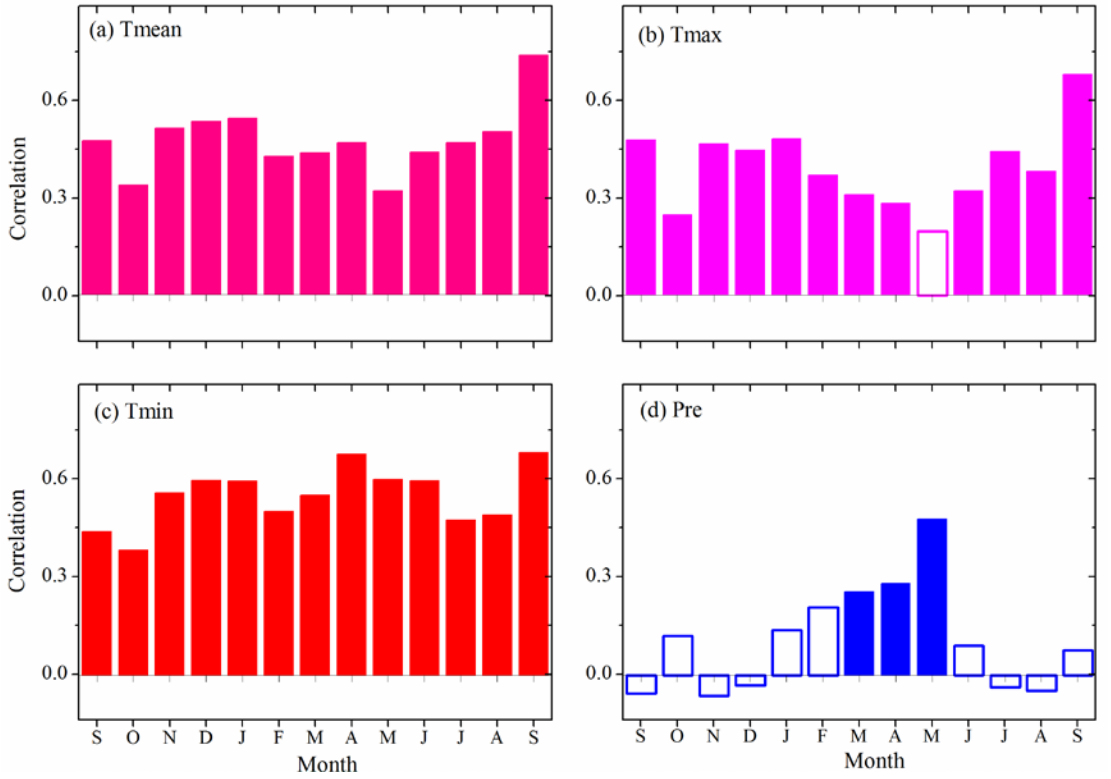

Fig.3 Bootstrap correlations between LOS and climate factors from previous September to current September over the period 1960–2014. (a) correlations with mean temperature (Tmean); (b) correlations with maximum temperature (Tmax); (c) correlations with minimum temperature (Tmin); (d) correlations with precipitation (Pre). The insignificant ($p > 0.05$) correlations are marked with hollow histogram, while the significant ($p < 0.05$) correlations are demonstrated with filled color bars.

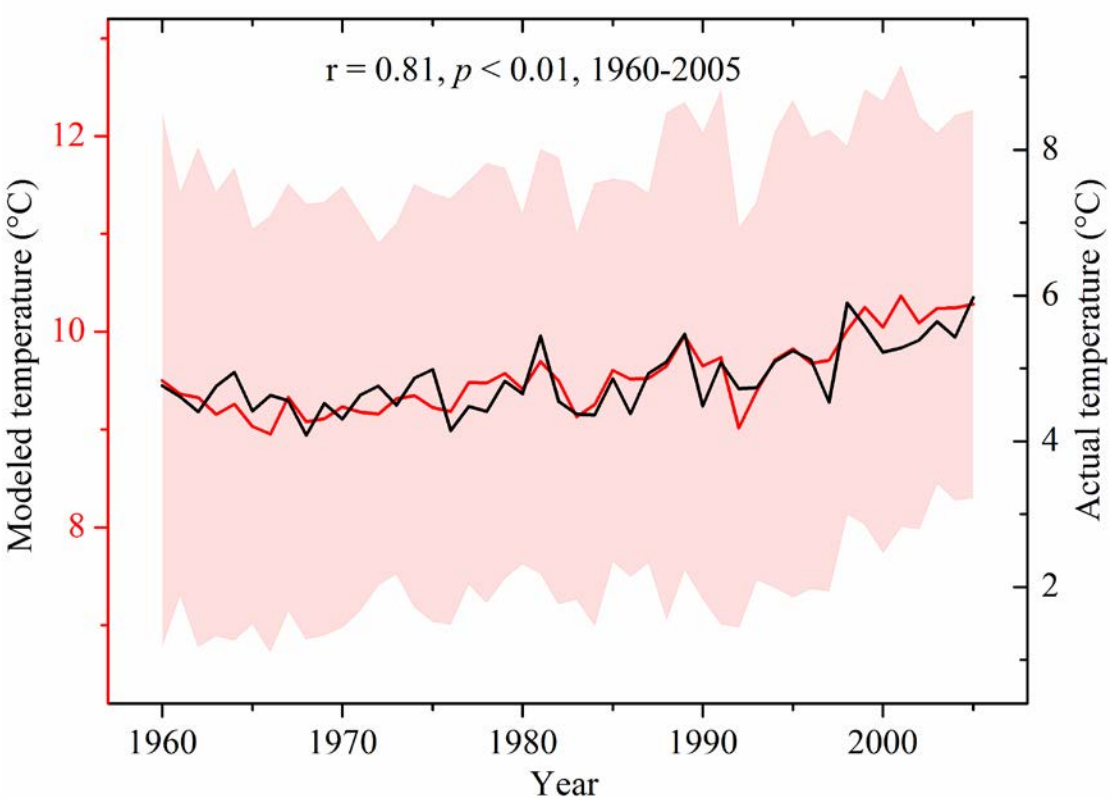

Fig.4 Comparison of the observed (black line) April–September minimum temperatures with results simulated (red line) by climate models under the historical period 1960–2005. Pink shaded bands show the 5% to 95% uncertainty range for these simulations from the 17 climate models.

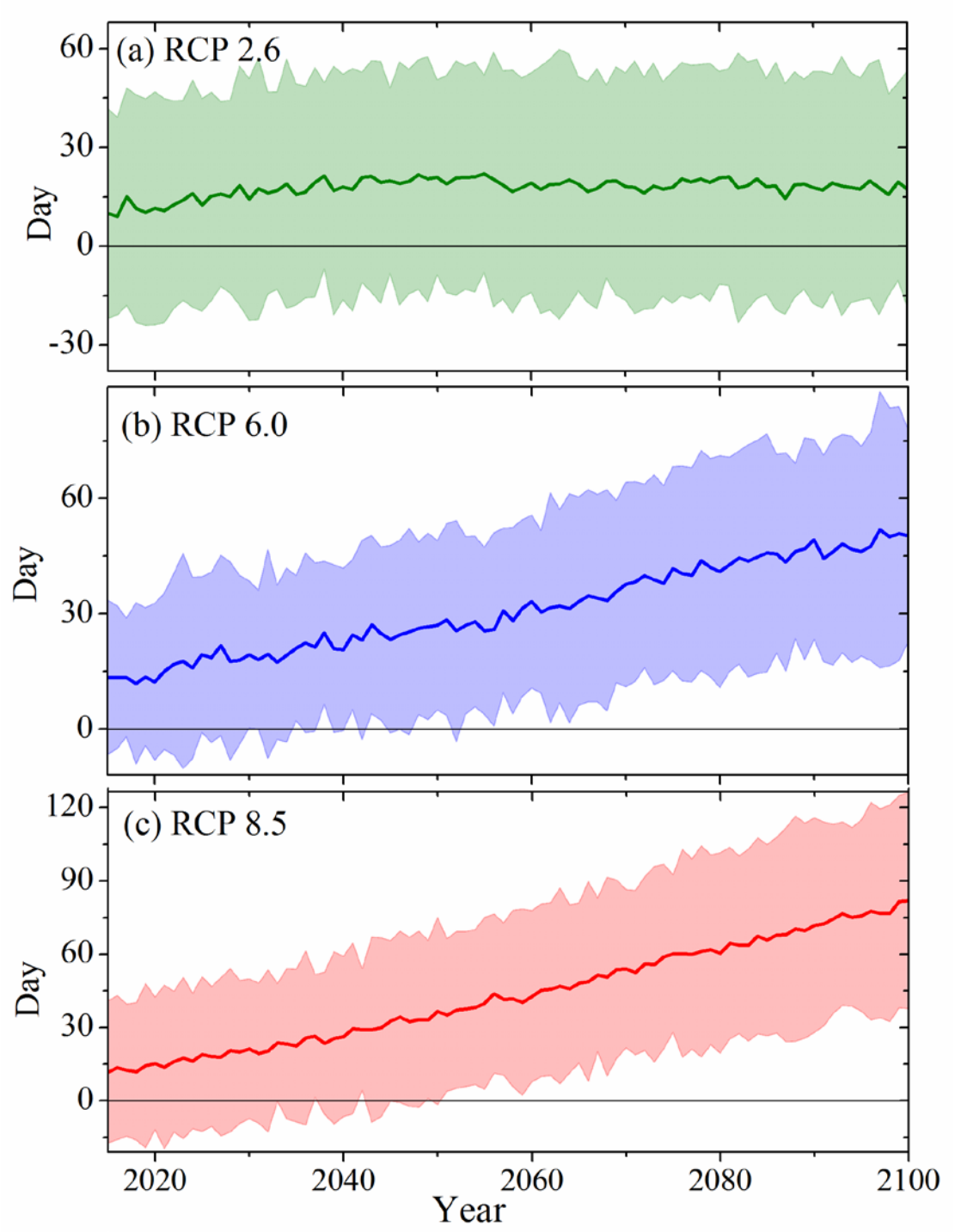

Fig.5 LOS time series averaged over the Tibetan Plateau during 2015–2100 with respect to 1960–2014, projected by the CMIP5 models under the RCP 2.6, RCP 6.0, and RCP 8.5 scenarios. Negative (positive) values indicate the reduction (extension) in the number of days with respect to 1960–2014. The different colored shaded bands show the 5% to 95% uncertainty range for these simulations under the three RCP scenarios.

Table 1 Details of the CMIP5 models used in this study.

Model name	Group	RCP 2.6	RCP 6.0	RCP 8.5

1	ACCESS1-3	Commonwealth Scientific and Industrial Research Organization and Bureau of Meteorology, Australia	No	No	Yes
2	bcc-csm1-1-m	Beijing Climate Center, China Meteorological Administration	Yes	Yes	No
3	CCSM4	National Center for Atmospheric Research	Yes	Yes	Yes
4	CMCC-CMS	Centro Euro-Mediterraneo per I Cambiamenti Climatici	No	No	Yes
5	CSIRO-Mk3-6-0	Commonwealth Scientific and Industrial Research Organization, Queensland Climate Change Centre of Excellence	Yes	Yes	Yes
6	EC-EARTH	EC-EARTH consortium	Yes	No	Yes
7	FGOALS-g2	The National Key Laboratory of Numerical Modeling for Atmospheric Sciences and Geophysical Fluid Dynamics (LASG), Institute of Atmospheric Physics, CAS	Yes	No	Yes
8	FIO-ESM	The First Institute of Oceanography, SOA, China	Yes	Yes	Yes
9	GFDL-ESM2G	NOAA Geophysical Fluid Dynamics Laboratory	Yes	Yes	Yes
10	GFDL-ESM2M	NOAA Geophysical Fluid Dynamics Laboratory	Yes	Yes	Yes
11	GISS-E2-R-3	NASA Goddard Institute for Space Studies	Yes	Yes	Yes
12	HadGEM2-AO	National Institute of Meteorological Research/Korea Meteorological Administration	Yes	Yes	Yes
13	HadGEM2-ES	Meteorological Office Hadley Center, UK	Yes	Yes	Yes
14	MIROC5	Japan Agency for Marine-Earth Science and Technology, Atmosphere and Ocean Research Institute, and National Institute for Environmental Studies	Yes	Yes	Yes
15	MIROC-ESM	Japan Agency for Marine-Earth Science and Technology, Atmosphere and Ocean Research Institute, and National Institute for Environmental Studies	Yes	Yes	Yes
16	NorESM1-M	Norwegian Climate Centre	Yes	Yes	Yes
17	NorESM1-ME	Norwegian Climate Centre	Yes	Yes	Yes

GISS-E2-R-3 means GISS-E2-R with the realization of _r1i1p3. Yes (No) indicates that the model is (is not) included under the respective RCP scenario.

Table 2 Predicted LOS time series averaged (± standard deviation) over the Tibetan Plateau during 2015–2100 with respect to 1960–2014, projected by the CMIP5 models under the RCP 2.6, RCP 6.0 and RCP 8.5 scenarios.

	RCP 2.6	RCP 6.0	RCP 8.5
2015–2040	14.98 ± 3.18	17.85 ± 3.42	19.08 ± 4.66
2041–2060	19.83 ± 1.48	26.84 ± 2.61	35.91 ± 4.77
2061–2080	18.69 ± 1.35	36.92 ± 4.08	53.89 ± 5.82
2081–2100	18.21 ± 1.50	46.78 ± 2.59	72.06 ± 5.65
Ensemble mean	17.72 ± 2.83	31.10 ± 11.57	43.41 ± 20.96

673

674 **Table 3** Predicted vegetation growing season by other studies.

Study region	Baseline period	Predicted period	Extension	Reference
Czech Republic and Austria	1961–1990	2050	8–30 days	(Trnka et al., 2011)
Nordic Arctic	1961–2000	2050	21–28 days	(Førland et al., 2004)
China	1961–1990	2080s	100 days	(Tian et al., 2014)
The majority of Europe	1971–2000	late 21st century	45–60 days	(Ruosteenoja et al., 2016)
Finland	1971–2000	end of the 21st century	40–50 days	(Ruosteenoja et al., 2011)

675

676

677

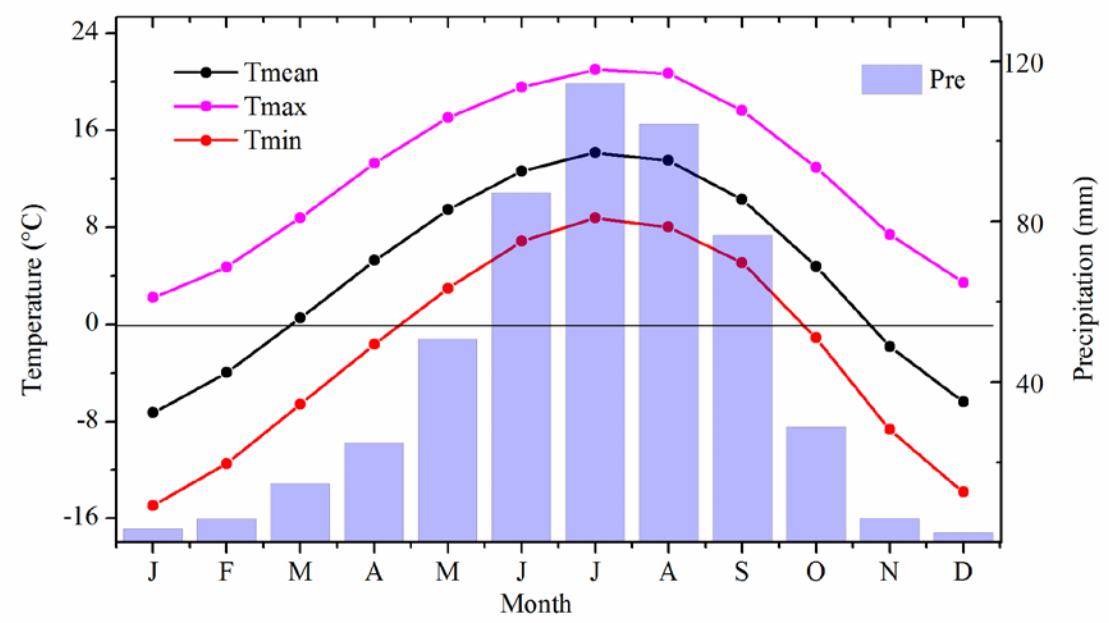

678

679 **Fig.S1** Monthly mean averaged climate conditions for the study region during the
680 period 1960–2014. Tmean, Tmax, and Tmin indicate mean temperature, mean
681 maximum temperature and mean minimum temperature, respectively. Pre means
682 precipitation.

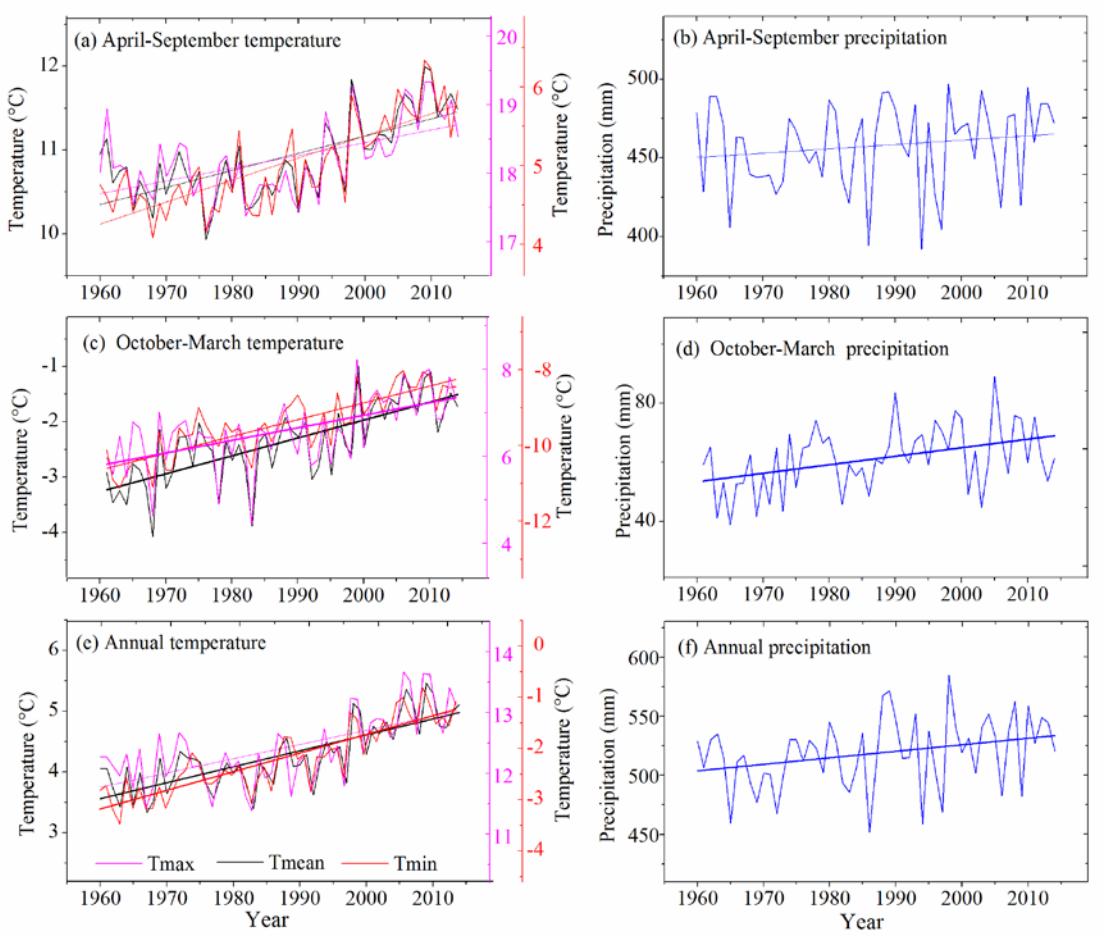

683

684 **Fig. S2** Characteristics of mean temperature (Tmean), mean maximum temperature
685 (Tmax), mean minimum temperature (Tmin) and precipitation during the past 55
686 years. The linear fitted series are also presented for the different climate factors during
687 1960–2014. Information for the detailed trends is listed in Table S1.

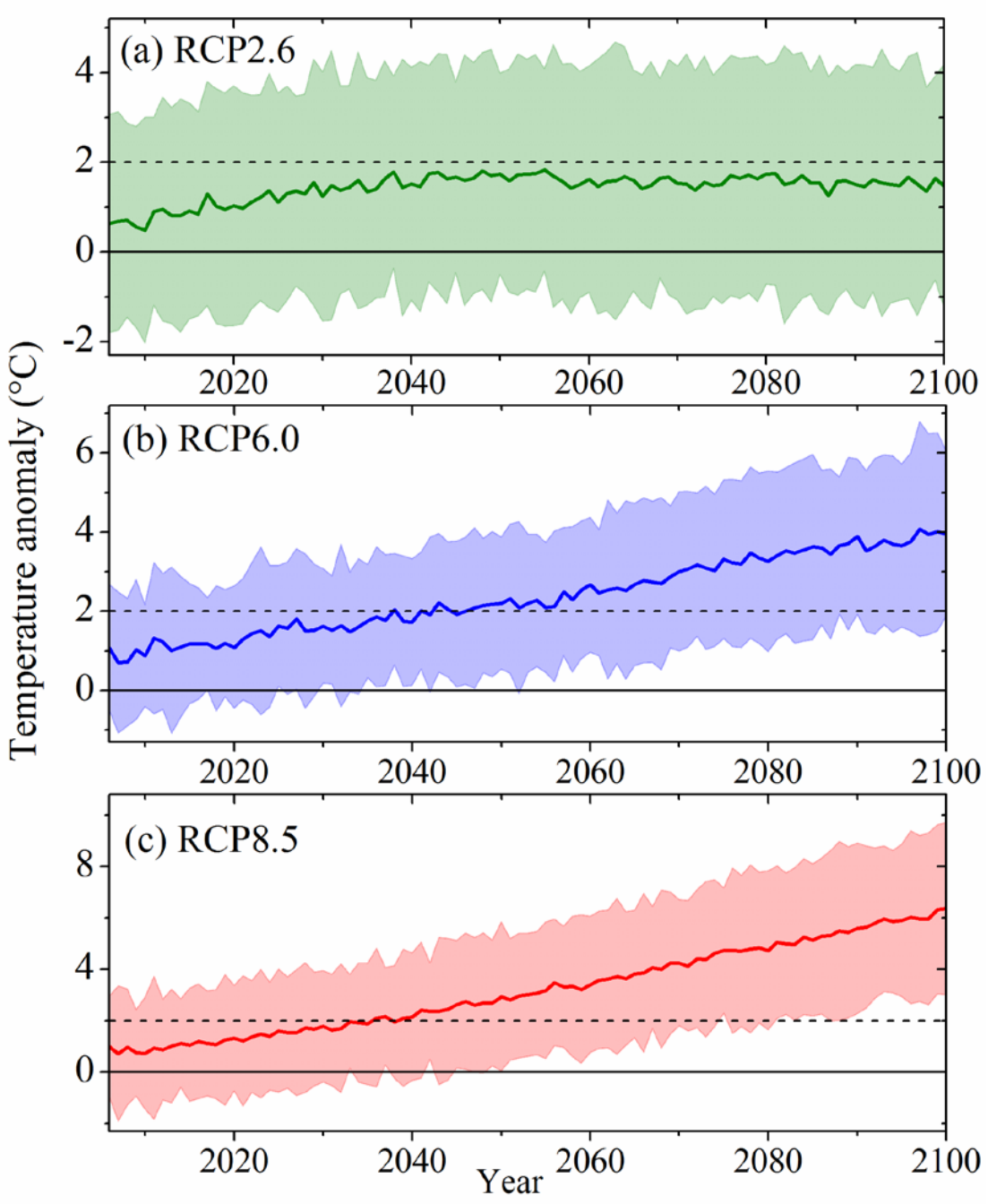

Fig.S3 Predicted April–September minimum temperature series under the three scenarios of RCP 2.6, RCP 6.0 and RCP 8.5 for 2006–2100. Temperature anomaly is calculated with respect to the "historical period" 1960–2005. The shaded bands show the 5% to 95% uncertainty range for these simulations under the three RCP scenarios.

Table S1 Linear trends of temperature and precipitation averaged from 20 meteorological stations data during the past 55 years (1960–2014) on the Tibetan Plateau (TP).

	April-September	October-March	Annual
Tmean	Slope = 0.020, $p < 0.01$, $R^2_{adj} = 0.45$	Slope = 0.033, $p < 0.01$, $R^2_{adj} = 0.52$	Slope = 0.026, $p < 0.01$, $R^2_{adj} = 0.60$
Tmax	Slope = 0.019, $p < 0.01$, $R^2_{adj} = 0.28$	Slope = 0.029, $p < 0.01$, $R^2_{adj} = 0.31$	Slope = 0.023, $p < 0.01$, $R^2_{adj} = 0.40$

Tmin	Slope = 0.028, $p < 0.01$, $R^2_{adj} = 0.61$	Slope = 0.044, $p < 0.01$, $R^2_{adj} = 0.70$	Slope = 0.036, $p < 0.01$, $R^2_{adj} = 0.75$
Pre	Slope = 0.276, $p = 0.23$, $R^2_{adj} = 0.01$	Slope = 0.288, $p < 0.01$, $R^2_{adj} = 0.16$	Slope = 0.550, $p = 0.03$, $R^2_{adj} = 0.07$

Tmean denotes the mean temperature; Tmax denotes the mean maximum temperature; Tmin denotes the mean minimum temperature; Pre denotes precipitation.

Table S2 Predicted April–September minimum temperature over the TP for the period 2006–2100 with respect to 1960–2005 (historical scenario), projected by the CMIP5 models under the RCP 2.6, RCP 6.0 and RCP 8.5 scenarios.

	2006–2020	2021–2040	2041–2060	2061–2080	2081–2100
RCP 2.6	0.84	1.38	1.66	1.58	1.54
Lower limit	-1.59	-1.13	-0.93	-1.11	-1.12
Upper limit	3.28	3.89	4.26	4.26	4.20
RCP 6.0	1.07	1.62	2.19	2.95	3.70
Lower limit	-0.54	-0.05	0.40	0.92	1.50
Upper limit	2.67	3.29	3.98	4.99	5.89
RCP 8.5	1.00	1.74	2.88	4.24	5.61
Lower limit	-1.18	-0.58	0.31	1.42	2.49
Upper limit	3.17	4.06	5.44	7.05	8.73

The lower and upper limits indicate the 5%–95% uncertainty intervals calculated from the multiple models.